Sign Regressor Least Mean Square Control Algorithm and Adaptive P&O Algorithm for Single Stage PV System Integrated with Power Grid

Chintapalli Satya Praneeta[1], M Srinivasarao[2]

[1]*PG Student, Department of EEE, Bonam Venkata Chalamayya engineering college, Odalarevu, Andhra Pradesh, India.*

[2]*Professor, Department of EEE, Bonam Venkata Chalamayya engineering college, Odalarevu, Andhra Pradesh, India.*

Corresponding Author: *cspraneeta303@gmail.com*

Abstract: -The project work proposes sign regressor least mean square (LMS) algorithm with P&O algorithm for single stage grid-connected solar PV generator system. For grid synchronization, the proposed algorithm adaptive filtering-based method is designed for DC to AC conversion with required rated frequency and voltage values as well as abc phase sequence. The algorithm also seeks to include features like harmonic correction and VAR generation, load balancing, and adaptive DC link voltage regulation, among others. Additionally, to reduce number of stages in grid-connected solar PV generator system, adaptive P&O algorithm proposed. A single-stage three-phase grid connected PV system is used to test the adaptive algorithm with linear as well as non-linear loads. The system is simulated in MATLAB with Simulink toolbox. Simulation results obtained show the effectiveness of the applied algorithm under steady and dynamic state operations.

Key Words:—*Solar Photo voltaic, HCC, MPPT, LMS.*

I. INTRODUCTION

Renewable energy (RE) is being hailed as the solution for combating global warming, climate change, and the continuous depletion of fossil resources. As a result, researchers, government agencies, and utilities are working together to incorporate renewable energy sources into the power grid and distribution networks. [1]. Solar energy is the best source of renewable energy in the current context since it is clean, noiseless, non-polluting, and abundant even in remote areas. Voltage instability, reliability, a poor grid infrastructure, and degraded power quality are some of the primary potential issues when integrating solar photovoltaic (SPV) systems with the grid [1]. The SPV system has shown to be a cutting-edge technology in the world of power systems, since it has proven to be very efficient in giving electricity to remote locations where transmission networks cannot reach, as well as being simple to install, minimal maintenance, and having a variety of other benefits.

Manuscript revised November 23, 2021; accepted November 24, 2021. Date of publication November 25, 2021.

This paper available online at www.ijprse.com

ISSN (Online): 2582-7898; SJIF: 5.494

The first stage of a traditional double-stage topology entails maximum power point tracking, while the second stage regulates the extracted power into the distribution network. Barnes et al. [2] have shown that for systems with DC link voltage larger than 340 V, a single stage design is more effective than a double stage topology. In single phase systems, single stage architecture has demonstrated its capability, resulting in significant losses decrease.

For grid integrated PV systems operating under abnormal grid conditions [3], using 12-pulse VSC [4], dual-purpose mode [5], and with frequency control [6,] some single-stage topologies have already been reported. Furthermore, various MPPT (Maximum Power Point Tracking) techniques have been discussed and compared in the literature [7], including hill climbing or P&O, fuzzy logic control, incremental conductance, neural network, FOCV (Fractional Open Circuit Voltage), FSCI (Fractional Short Circuit Current), and so on.

Artificial bee colony (ABC) control method [8] and improved MPPT controller under partial shading conditions [9] are two new advanced MPPT techniques. The P&O technique for MPPT can be implemented in two ways, depending on the control parameters used, such as reference voltage and duty ratio, as detailed in [10-11]. Transferring reactive power to

great distances from the grid to meet load requirements has been found to be a very ineffective undertaking.

As a result, SPV generating equipment can be placed close to the load for reactive load correction. SRFT (Synchronous Reference Frame Theory) [12], IRPT Voltage distortions may cause erroneous tripping of VSC controllers and power electronic switches (PES), affecting system performance during transition modes.

THD of generating voltages, generator currents, grid voltages, and grid currents has been defined by standards such as IEEE 519 [28]. [29] discusses a control technique for eliminating current harmonics and, as a result, lowering grid supply THD.

The VSC, on the other hand, lacks the capacity to effortlessly switch between grid and islanded modes. The authors have only discussed smooth transition without improving power quality in all of these works on reconfigurable microgrids (seamless transition) (PQI). The authors have exclusively considered an inverter-based DC voltage generation system in these papers. There is no attempt to describe what would happen if the reconfigurable system consisted of a mix of direct AC (small hydro) and inverter-based DC generation.

II. CONTROL TECHNIQUE

The single-stage three-phase system considered for the present study consists of two control algorithms, one for extract reference DC voltage and another for VSC. P&O algorithm controls the reference DC voltage. Novel SRLMS adaptive algorithm is used for UPF operation of VSC.

2.1 P&O Algorithm

The flowchart for the solar MPP scheme is shown in Figure 1. By introducing a changeable perturbation step size, the adaptive P&O MPP control solves the oscillations difficulties of fixed step based MPP approaches.

Using a product of short circuit current and ideal proportionality constant [36], the control calculates the MPP operating point. The perturbation step size tuning process is based on irradiance level and operating point oscillations around the power maxima, which are referred to as coarse and fine tuning, respectively.

The insolation level of a solar PV array defines the perturbation size for coarse tuning, whereas the oscillations around the MPP determine the perturbation size for fine tuning.

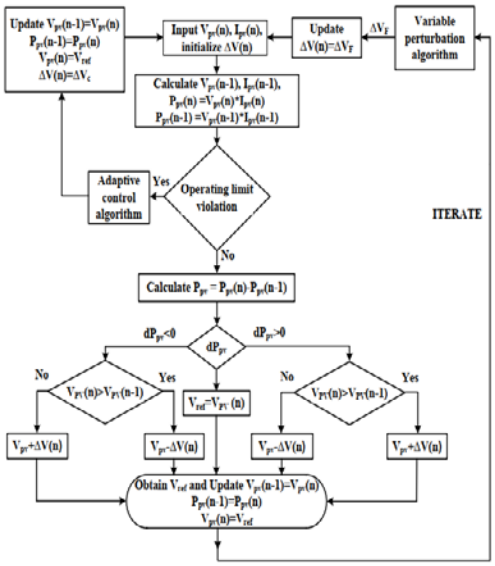

Fig.1. Flowchart for Perturb and Observe MPPT algorithm

2.2 Proposed control Algorithm

The proposed SRLMS algorithm schematic diagram is shown in Fig.2. The sensed signals for the proposed algorithm are: load currents ila, ilb and ilc; PCC voltages vta, vtb and vtc; grid currents isa, isb and isc; and DC-link voltage Vdc. These signals are fed to the controller for extraction of reference currents $(i_{sa}^*, i_{sb}^*, i_{sc}^*)$ which leads to switching gate pulse signal generation for the VSC. The SRLMS-based adaptive control technique can be separated into three elements, as indicated in fig. 2, namely network synchronization control, voltage control, and gating pulse generation control. The voltage across the DC-link capacitor is regulated by comparing the detected and reference values of DC-link voltage in the upper section, referred to as voltage control. It employs controllers to force the real quantity to match the reference value. The voltage error signal (ve) is processed by a traditional PI controller to provide 'wloss,' a current component that is added to the reference current signals generated by network synchronisation control to compensate for any energy imbalance in the DC-link.

$$w_{loss}(n) = w_{loss}(n-1) + K_p\{v_e(n) - v_e(n-1)\} + K_i v_e(n) \quad (1)$$

where, K_p and K_i are gains of PI controller, *wloss* is an active loss component of VSC, and v_e is the voltage error signal $(V_{dc}^* - V_{dc})$ Network synchronization control extracts the fundamental component of the control signal (i_s^*) by processing the sensed signals. The in-phase (p) and in

quadrature (q) unit vectors of the terminal voltages (Vt) are calculated using magnitude Vt, and are given by

$$V_t = \sqrt{\frac{2}{3}(V_{ta}^2 + V_{tb}^2 + V_{tc}^2)} \quad (2)$$

$$p_a = v_{ta} / v_t$$
$$p_b = v_{tb} / v_t$$
$$p_c = v_{tc} / v_t \quad (3)$$

$$q_a = (p_a - p_b)/\sqrt{3}$$
$$q_b = \sqrt{3}p_a / 2 + (p_b - p_c)/2\sqrt{3}$$
$$q_c = -\sqrt{3}p_a / 2 + (p_b - p_c)/2\sqrt{3} \quad (4)$$

Because VSC is used in UPF mode in this study, only in-phase unit vectors are required for active power control. The SRLMS-based control algorithm calculates the weights (wpa, wpb, and wpc) for active power components of load currents. The objective here is to minimize. mean square error. And, it is achieved by iteratively updating the weights by updation rule which is given by,

$$w_{pa}(k+1) = w_{pq}(k) + 2\gamma e_a \{sign(p_a(k))\} \quad (5)$$

Where, γ is step size and *ea (k)* is error defined as,

$$e_a(k) = i_{La}(k) - p_a(k)w_{pa}(k) \quad (6)$$

Where, i_{La} *(k)* is the sensed load current of '*a*' phase at the k[th] instant. Similar computations can be made for the active weights of phase '*b*' and phase '*c*' load currents. Average active weight of load currents (w_{avg}) is calculated as,

$$w_{avg} = (w_{pa} + w_{pb} + w_{pc})/3 \quad (7)$$

to grid

The total active weight from voltage control and network synchronization control is given as

$$w_p = w_{loss} + w_{avg} \quad (8)$$

The computed weights are then utilized to generate reference grid currents and are given by

$$i_{sa}^* = w_p p_a$$
$$i_{sb}^* = w_p p_b$$
$$i_{sc}^* = w_p p_c \quad (9)$$

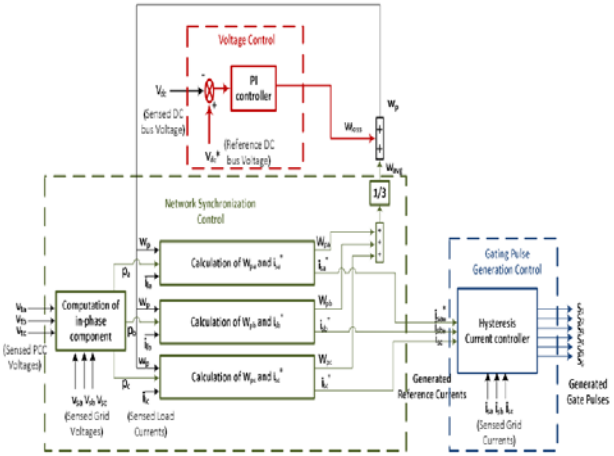

Fig. 2. Schematic of proposed SRLMS based adaptive control algorithm for VSC control of PV generator system connected to grid.

The final section, gating pulse generation control, is made up of a hysteresis current controller (HCC) that analyses the signals of measured and generated reference grid currents in order to generate VSC gating pulses. The reference current signals are used to construct a band that controls the sensed current. If the measured current exceeds the band's upper limit, the controller reduces it by activating the negative voltage switching mechanism. If the perceived current exceeds the band's lower limit, the controller activates the positive voltage switching function, which increases the sensed current. The six gate pulses generated are delivered to the VSC.

III. PROPOSED SYSTEM

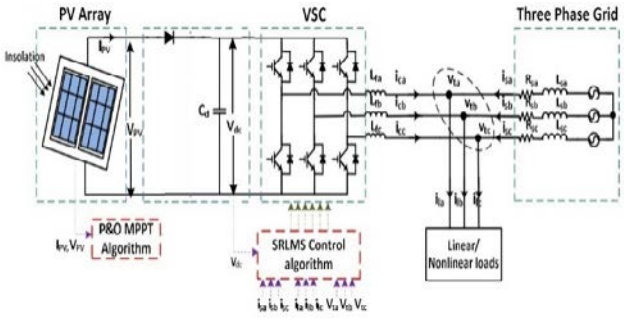

Fig.3. Proposed System

The system configuration given here is for a 30 kW SPV system connected to a three-phase grid with the loads depicted in Fig. 1. SPV array, linear and nonlinear loads, DC bus voltage, DC link capacitance, IGBT (Insulated Gate Bipolar Transistor) based VSC rating, interfacing inductances, and the ripple filter are among the system components to be designed. [22] discusses various models of SPV modules. Villava et al. [22] provided a method for modelling an SPV array, which is

used to construct and model an SPV array in this study. Figure 2 shows the details of the SPV array model that was chosen. The SPV array employed in this study is designed for a maximum power capacity of 30 kW when linked to a 3 phase, 415 V, 50 Hz system. The number of SPV modules in series is predicted to be as follows:

$$n_s = \frac{V_{dc}}{V_{mp}} = \frac{700}{26.3} = 26.7\, or\, 27\, modules \quad (10)$$

The number of SPV modules connected in parallel are estimated as,

$$n_p = \frac{p_{\max} / V_{dc}}{I_{mp}} = \frac{3000/700}{7.61} = 5.63\, or\, 6\, modules \quad (11)$$

As a result, the SPV array with a peak power capacity of 30 kW is modelled using 27 series modules and 6 parallel modules.

The minimum DC bus voltage that must be maintained for the VSC must be more than double the peak phase voltage at the PCC (Point of Common Coupling) or the grid. As a result, [23] is used to calculate the DC bus voltage.

$$V_{dc} = \frac{2\sqrt{2}V_{LL}}{\sqrt{3}\times m} = \frac{2\sqrt{2}\times 415}{\sqrt{3}\times 1} = 677.69V \quad (12)$$

Where, V_{LL} is grid line voltage and m is the modulation index. (Values considered here are m=1 and V_{LL}=415 V). So, the value of Vdc is taken as 700 V.

IV. RESULTS AND DISCUSSION

The study's system is modelled in MATLAB with the Simulink toolkit. The appendix contains a list of the parameters used in the simulation. The solar PV generator system consists of a 10 kW PV array, a boost converter, and a VSC that connects the system to the grid. The gating pulses for VSC are generated by the suggested algorithm. To investigate the performance of the proposed algorithm under simulated steady-state and dynamic state settings, linear and non-linear loads are attached to the system.

4.1 Proposed control algorithm performance under balanced linear load

The proposed based adaptive control algorithm's simulation results under balanced three-phase linear load conditions are shown in Fig. 4. The algorithm's UPF control action in a grid-connected system is tested using a 20 kVA inductive linear load with a 0.8 power factor lag. The load's reactive power need is met locally by the VSC, which reduces the grid's reactive power demand to zero. The voltages and currents on the grid are in phase. Furthermore, the grid current THD is 3.04 percent, which is well within the IEEE 519-2014 norm [19]. As a result, the suggested algorithm can successfully run the VSC in UPF mode while preserving the power flow balance in the grid-connected solar PV generator system.

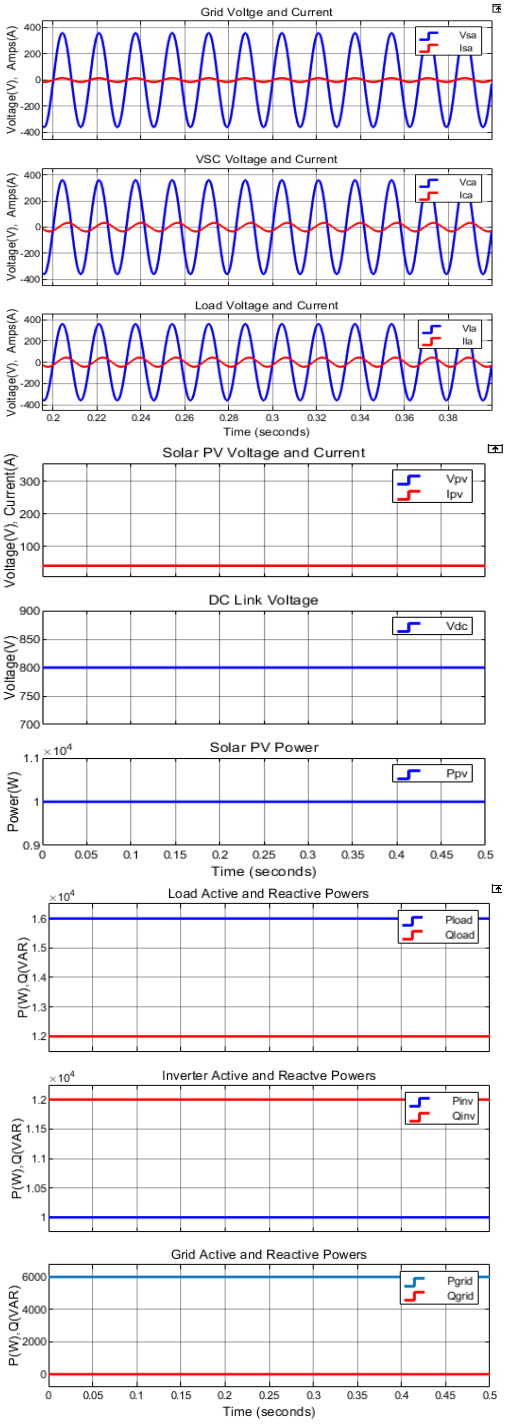

Fig.4. Simulation results of proposed control algorithm under balanced linear load

4.2 Proposed control algorithm performance under unbalanced non-linear load

The SRLMS-based adaptive control technique for non-linear load under load unbalancing conditions is shown in Fig. 5. A three-phase diode bridge rectifier with RL load (10, 0.8 mH) is connected as a non-linear load. When the load in phase 'a' reaches zero, VSC takes necessary action and begins drawing equal and opposite current from the grid. As a result, the load and VSC together appear to be a balanced three-phase load to the grid from the grid's perspective. Grid currents in all phases have stabilized at 8.4 A per phase, down from a peak of 26.5 A per phase. In addition, i_{sa} remains in phase with v_{sa}, ensuring that the UPF operation is legitimate.

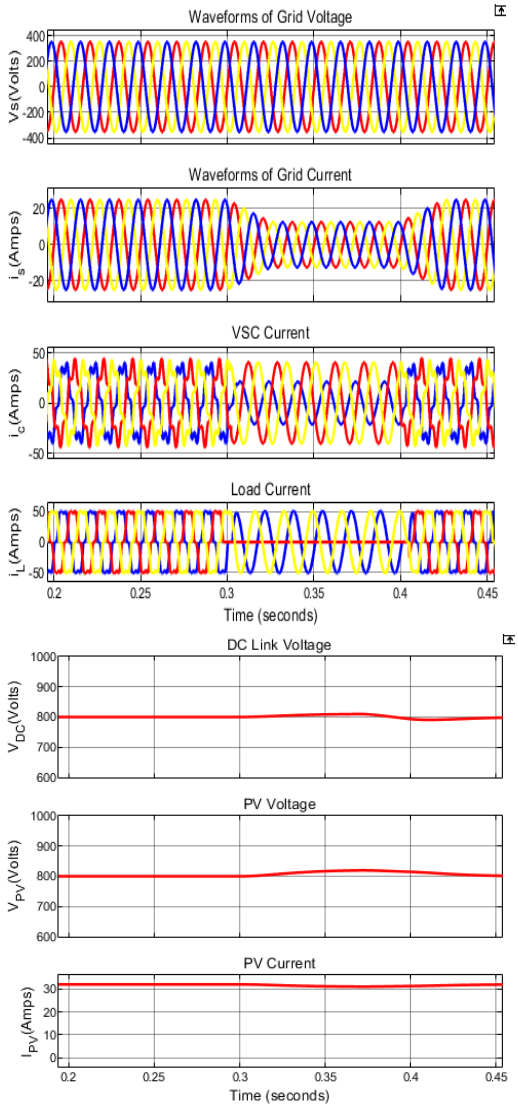

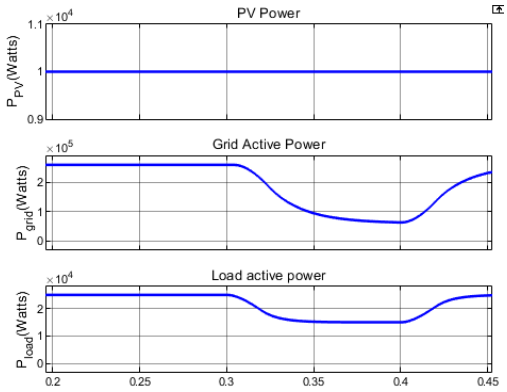

Fig.5. Simulation results of proposed control algorithm under unbalanced linear load

V. CONCLUSION

This research proposes a unique sign regressor LMS based adaptive control technique for solar PV generator systems connected to the grid. The simulation findings show that it performs well in UPF mode in both a steady and dynamic state of operation, such as irradiation variation and load unbalancing at PCC. THD levels of PCC voltage and grid current are maintained according to IEEE-519 standards, ensuring that power quality criteria are met with both linear and non-linear loads. The suggested adaptive algorithm also offers additional functionalities of VAR production, harmonic correction, adaptive DC-link voltage regulation, and load balancing, in addition to preserving the grid-connected system's power balance, according to simulation findings.

REFERENCES

[1]. A. M. Bouzid, J. M. Guerrero, A. Cheriti, M. Bouhamida, P. Sicard, and M. Benghanem, “A survey on control of electric power distributed Generation systems for microgrid applications applications,” Renewable and Sustainable Energy Reviews, vol. 44, pp. 751-766, Apr. 2015.

[2]. I. Patrao, E. Figueres, G. Garcera, and R. Gonzalez-Medina, “Microgrid architectures for low voltage distributed generation,” Renewable and Sustainable Energy Reviews, vol. 43, pp. 415-422, Mar. 2015.

[3]. IEEE Std. 1547-2003, “Standard for interconnecting distributed resources with electric power systems,” IEEE, ISBN 0-7381-3720-0SH95144, Jun. 2003.

[4]. S. Chung, “A phase tracking system for three phase utility interface inverters,” IEEE Trans. Power Electr., vol. 15, no. 3, pp. 431 – 438, May. 2000.

[5]. F. Blaabjerg, R. Teodorescu, M. Liserre, and A. V. Timbus, "Overview of control and grid synchronization for distributed power generation systems," IEEE Trans. Indus. Electron., vol. 53, no. 5, pp. 1398-1409, Oct. 2006.

[6]. E. Robles, S. Ceballos, J. Pou, J. L. Martin, J. Zaragoza, and P. Ibanez, "Variable-frequency grid-sequence detector based on a quasi-ideal lowpass filter stage and a phase-locked loop," IEEE Trans. Power Electr., vol. 25, no. 10, pp. 2552 – 2563, Oct. 2010.

[7]. F. Freijedo, J. Doval-Gandoy, O. Lopez, and E. Acha, "A generic openloop algorithm for three-phase grid voltage/current synchronization with particular reference to phase, frequency, and amplitude estimation," IEEE Trans. Power Electr., vol. 24, no. 1, pp. 94-107, Jan. 2009.

[8]. S. Golestan, J. M. Guerrero, and A. M. Abusorrah, "MAF-PLL with phase-lead compensator," IEEE Trans. Indus. Electron., vol. 62, no. 6, pp. 3691-3695, Jun. 2015.

[9]. Z. Yao, L. Xiao, and J. M. Guerrero, "Improved control strategy for the three-phase grid-connected inverter," IET Renewable Power Generation, vol. 9, no. 6, pp. 587 – 592, Jan. 2015.

[10]. D. N. Zmood, and D. G. Holmes, "Stationary frame current regulation of PWM inverters with zero steady-state error," IEEE Trans. Power Electr., vol. 18, no. 3, pp. 814 – 822, May. 2003.

[11]. J. C. Vasquez, J. M. Guerrero, M. Savaghebi, J. Eloy-Garcia, and R.Teodorescu, "Modeling, analysis, and design of stationary-referenceframe droop-controlled parallel three-phase voltage source inverters," IEEE Trans. Indus. Electron., vol. 60, no. 4, pp. 1271 – 1280, Apr. 2013.

[12]. R. Teodorescu, F. Blaabjerg, M. Liserre, and P. C. Loh, "Proportionalresonant controllers and filters for grid-connected voltage-source converters," IEE Proceedings - Electric Power Applications, vol. 153, no. 5, pp. 750 – 762, Sep. 2006.

[13]. M. Castilla, J. Miret, A. Camacho, J. Matas, and L. G. de Vicuña, "Reduction of current harmonic distortion in three-phase grid-connected photovoltaic inverters via resonant current control," IEEE Trans. Indus. Electron., vol. 60, no. 4, pp. 1464 – 1472, Apr. 2013.

[14]. X. Yuan, W. Merk, H. Stemmler, and J. Allmeling, "Stationary-frame generalized integrators for current control of active power filters with zero steady-state error for current harmonics of concern under unbalanced and distorted operating conditions," IEEE Trans. Indus. Appl., vol. 38, no. 2, pp. 523 – 532, Mar. 2002.

[15]. M. Liserre, R. Teodorescu, and F. Blaabjerg, "Multiple harmonics control for three-phase grid converters systems with the use of PI-RES current controller in a rotating frame," IEEE Trans. Power Electr., vol. 21, no. 3, pp. 836 – 841, May 2006.

[16]. R. I. Bojoi, G. Griva, V. Bostan, M. Guerriero, F. Farina, and F. Profumo, "Current control strategy for power conditioners using sinusoidal signal integrators in synchronous reference frame," IEEE Trans. Power Electr., vol. 20, no. 6, pp. 1402 – 1412, Nov. 2005.

[17]. S. W. Kang and K. H. Kim, "Sliding mode harmonic compensation strategy for power quality improvement of a grid-connected inverter under distorted grid condition," IET Power Electr., vol. 8, no. 8, pp. 1461 – 1472, Feb. 2015.

[18]. Q. C. Zhong and T. Hornik, "Cascaded current-voltage control to improve the power quality for a grid-connected inverter with a local load," IEEE Trans. Indus. Electron., vol. 60, no. 4, pp. 1344 – 1355, Apr. 2013.

[19]. Y. Jia, J. Zhao, and X. Fu, "Direct grid current control of LCL-filtered grid-connected inverter mitigating grid voltage disturbance," IEEE Trans. Power Electr., vol. 29, no. 3, pp. 1532 – 1541, Mar. 2014.

[20]. Y. A. I. Mohamed, "Mitigating of dynamic, unbalanced, and harmonic voltage disturbance using grid-connected inverters with LCL filter," IEEE Trans. Indus. Electron., vol. 58, no. 9, pp. 3914 – 3924, Sep. 2011.